NOVA SCHOOL OF SCIENCE & TECHNOLOGY

DEPARTMENT OF PHYSICS

BEATRIZ CATARINO OLIVEIRA

BSc in Biomedical Engineering

MAGNESIUM-BASED BIODEGRADABLE SCAFFOLDS FOR BONE TISSUE REGENERATION

MASTER IN BIOMEDICAL ENGINEERING

NOVA University Lisbon
October, 2023

NOVA SCHOOL OF SCIENCE & TECHNOLOGY

DEPARTMENT OF PHYSICS

MAGNESIUM-BASED BIODEGRADABLE SCAFFOLDS FOR BONE TISSUE REGENERATION

BEATRIZ CATARINO OLIVEIRA

BSc in Biomedical Engineering

Adviser: Carla Sofia Monteiro de Moura
Assistant Researcher, Institute of Applied Research (i2A) and Centre for Rapid and Sustainable Product Development (CDRSP)

Co-adviser: Ana Catarina Bernardino Baptista
Researcher, NOVA University of Lisbon, School of Science and Technology (NOVA SST)

Examination Committee

Chair: Célia Maria Reis Henriques
Associate Professor, NOVA University Lisbon

Rapporteur: Ana Cristina Araújo Veloso
Coordinating Professor, Polytechnic Institute of Coimbra

Adviser: Carla Sofia Monteiro de Moura
Assistant Researcher, Institute of Applied Research (i2A) and Centre for Rapid and Sustainable Product Development (CDRSP)

MASTER IN BIOMEDICAL ENGINEERING

NOVA University Lisbon
October, 2023

Magnesium-based Biodegradable Scaffolds for Bone Tissue Regeneration

This document was created with the (pdf/Xe/Lua)LaTeX processor and the NOVAthesis template (v6.10.17) [1].

Acknowledgements

I would like to start expressing my deep gratitude to my thesis advisor, Doctor Carla Moura, for her invaluable guidance, support, and patience throughout this journey. Besides, a huge thanks for the many opportunities to, not only work in such an exciting and booming field, cooperating with so many good people, but also to be able to show my work to other persons.

I extend my profound thanks to my co-advisor, Professor Ana Baptista, for her insightful feedback and constructive suggestions that greatly contributed to the quality of this thesis.

A special thanks to my family for their love, encouragement, and belief in my capacities. Their support helped me so much throughout all these years.

I want, also, to acknowledge the contribution of my friends during these years for the unconditional help and for sharing so many good moments.

I would like to extend my gratitude to Joel and Sofia for sharing their time and knowledge, and for their encouragement, support, work, and motivation during these months.

A huge and unique thanks to my boyfriend, João Pedro, for his love, patience, kindness, and for always being there and make me feel "at home". His advice and knowledge helped me to finish this chapter of my academic journey.

Finally, I extend my profound appreciation to everyone who has provided assistance, in ways whether seen or unseen, contributing to the successful completion of my master's thesis.

”

“The journey of a thousand miles begins with one step.”

— Lao Tzu

(Philosopher and Writer)

Abstract

Bone, a remarkable tissue with the ability to naturally regenerate when slightly damaged, faces limitations when submitted to critical injuries that can inhibit its inherent healing process, necessitating external interventions like bone grafts, which present challenges, restricting their clinical application. Thus, biodegradable materials have gained importance to be used for bone replacement alternatives. These materials can be manipulated to obtain porous structures in several forms, promoting cell proliferation and adhesion while supporting the formation of new bone. Magnesium (Mg) emerges as an attractive biomaterial for these scenarios due to its biodegradability, mechanical properties similar to natural bone, and its predominant presence in bones, making it an ideal candidate for bone applications. The primary goal of this study was to manufacture temporary implants for bone regeneration. Three approaches were studied incorporating Mg to achieve this: *i)* three-dimensional (3D) Additive Manufactured (AM) scaffolds; *ii)* hydrogels; and *iii)* hybrid, through the combination of a scaffold with hydrogel. To produce the AM scaffolds, two weight percentages of Mg, 5 and 15%, were used in two forms, Magnesium Oxide, MgO, and Magnesium Sulphate, $MgSO_4$. The addition of Mg resulted in a rough surface and enhanced mechanical properties, with an optimal Mg content of 5%, presenting the highest resistance to compression. A synthetic polymer, PEGDA, was used as the hydrogel base, and $MgSO_4$ was added. The mechanical properties of the Mg group showed an improvement in the compressive Young's Modulus (2.28 MPa) and an increase in their ductility. The plateau reached after an intital weight increase proved that these hydrogels do not degrade immediately, being stable enough to help bone regeneration. A third approach was made, combining the two previously mentioned, an AM scaffold with a Mg-hydrogel. Notably, the mechanical properties of this strategy surpassed those of both previous approaches. The results demonstrated that the hybrid approach presents a mechanical behaviour closer to the levels found in natural bone, reaching Compressive Young's Modulus of about 2 GPa.

Keywords: Bone Regeneration, Additive Manufactured Scaffolds, Hydrogel, Magnesium, Tissue Engineering

Resumo

O osso é um tecido com capacidade de se regenerar naturalmente quando ligeiramente danificado, mas enfrenta limitações quando sujeito a lesões críticas que podem inibir esta capacidade, tornando-se necessária intervenção externa, como enxertos ósseos, que apresentam alguns desafios. Assim, os materiais biodegradáveis têm ganho importância, podendo ser manipulados por forma a obter estruturas que promovem a proliferação e adesão celulares, enquanto suportam a formação de novo osso. O magnésio (Mg) surge como um biomaterial atrativo para estas situações por ser biodegradável, apresentar propriedades mecânicas semelhantes às do osso natural e ainda pela sua presença predominante nos ossos. O principal objetivo deste estudo foi fabricar implantes temporários para a regeneração óssea. Foram estudadas três abordagens, com a incorporação de Mg, para atingir este objetivo: *i)* estruturas tridimensionais (3D), scaffolds, produzidas por fabricação aditiva (AM); *ii)* hidrogéis; e *iii)* uma abordagem híbrida, através da combinação de um scaffold com um hidrogel. Para produzir os scaffolds, duas percentagens de Mg, 5 e 15%, foram usadas em duas formas diferentes, Óxido de Magnésio, MgO, e Sulfato de Magnésio, $MgSO_4$. A adição de Mg resultou numa superfície mais rugosa e melhorou as propriedades mecânicas, tendo o grupo de 5% Mg sido eleito como ótimo, apresentando a maior resistência à compressão. Um polímero sintético, PEGDA, foi usado em combinação com $MgSO_4$ para formulação do hidrogel. A adição de Mg levou a uma melhoria no módulo de compressão (2.28 MPa) e a um aumento da ductilidade. O *plateau* atingido após o aumento inicial da massa no teste de degradação comprovou que estes não se degradam imediatamente, sendo estáveis para auxiliar no processo de regeneração óssea. Foi ainda realizada uma terceira abordagem, combinando as estruturas anteriores, scaffold e hidrogel de Mg. Notavelmente, as propriedades mecânicas dessa estratégia superaram as das abordagens anteriores, apresentando um comportamento mecânico mais próximo dos níveis encontrados no osso natural, atingindo um módulo de compressão de quase 2 GPa.

Palavras-chave: Regeneração óssea, Scaffolds de Fabricação Aditiva, Hidrogel, Magnésio, Engenharia de Tecidos

Contents

List of Figures

List of Tables

Abbreviations

3D	Three-dimensional
AM	Additive Manufacturing
ECM	Extracellular Matrix
EDS	Energy-Dispersive X-ray Spectroscopy
FDM	Fused Deposition Modelling
FTIR	Fourier-Transform Infrared Spectroscopy
Mg^{2+}	Cation of Magnesium, with charge 2+
$Mg(OH)_2$	Magnesium Hydroxide
MgO	Magnesium Oxide
$MgSO_4$	Magnesium Sulphate
PCL	Poly(ϵ-caprolactone)
PEGDA	Polyethyleneglycol diacrylate
RT	Room Temperature
SC	Solvent Casting
SEM	Scanning Electron Microscopy
TE	Tissue Engineering
UV	Ultraviolet
wt	weight

XRD X-Ray Diffraction

1

Introduction

Tissue Engineering (TE) has emerged as a pivotal field, pioneering innovative solutions for tissue and organ regeneration [2, 3]. Among these organs, bone holds vital importance due to its role in locomotion, protection, mechanical adaptability, and support. Despite its inherent capacity for self-healing after minor damage, significant injury from diseases or injuries often results in critical-size lesions that cannot self-repair naturally [4]. In such cases, bone replacements are imperative [4]. Common approaches include autologous bone grafting, a widely used method [5], and allografts, which address certain limitations but introduce new challenges [6], including size restrictions, immune responses, limited availability, and the potential for disease transmission [7], thereby limiting their clinical utility.

There has been an increasing focus on biodegradable artificial implants made from synthetic biomaterials to address these limitations and enhance bone regeneration. These materials offer advantages over permanent implants due to their natural degradation after fulfilling their intended purpose [4]. Additionally, they can promote cell differentiation and support the deposition of new bone tissue [8]. The ideal synthetic biomaterials for bone substitutes should possess biocompatibility, mirror natural bone's extracellular matrix (ECM), facilitate complete bone regeneration, and degrade alongside new bone formation.

Mg, an abundant mineral mainly stored in bones, has emerged as a promising candidate for orthopaedic implants due to its biocompatibility and mechanical properties that resemble bone [9, 10]. Notably, Mg is biodegradable under physiological conditions, eliminating the need for additional surgeries to implant removal [11]. However, Mg's rapid corrosion rate poses challenges, impacting implant mechanical strength and hindering tissue healing. Strategies like surface modifications or material combinations can optimise corrosion rates [12]. Mg degradation releases Mg^{2+}, promoting bone formation, regulating cell behaviour [13], and enhancing osteoblast attachment [14]. Deficiency of this ion can disrupt skeletal metabolism, while excessive Mg^{+2} inhibits ECM formation [15, 16]. So, achieving optimal Mg levels is crucial.

Additive Manufacturing has revolutionised biomaterials for TE, particularly in bone

tissue regeneration, enabling the creation of customised structures with vital pore interconnectivity for cell migration and proliferation [17–19]. Before additive manufacturing, conventional techniques such as sol-gel [20], gas foaming [21] or freeze-drying [22] were used. Nonetheless, the lack of ability to have full control over the implant's architecture made this type of scaffold manufacturing a preferable type of process to provide not only personalise overall shape but also to manipulate the internal framework of the implant.

Fused Deposition Modelling (FDM), alternatively known as extrusion-based technique, stands as the prevailing 3D printing method for crafting composite scaffolds. Within this category of processing techniques, materials are manipulated in the form of filaments or paste. This involves loading the material into a nozzle, which is then affixed to a robotic arm responsible for executing the defined path generated by the slicer software. The material is subsequently dispensed from the nozzle by applying heat or pressure. This technique holds widespread usage due to its capacity to print a diverse range of materials cost-effectively while maintaining accuracy. Scaffolds produced through FDM exhibit interconnected pores coupled with substantial porosity [7, 23]. The scaffold's porosity significantly aids in cell migration, proliferation, and the vascularisation of emerging tissue [3, 24].

Besides AM scaffolds, other techniques and forms for bone replacements offered by TE also appear. The hydrogels, a form of polymeric scaffolds, are also emerging as a captivating substitute for bone. These hydrogels not only establish a conducive 3D environment, fostering cellular proliferation, adhesion, migration, and differentiation but also aid in restoring the functional integrity of bone imperfections [10]. They exhibit remarkable water absorption capacity and exceptional biomimetic traits as they strive to emulate the natural ECM environment. They typically function as carriers for bioactive ions, molecules, cells, and drugs, as they allow a rapid diffusion of metabolites and nutrients [10, 25, 26].

Some of these hydrogels are derived through the photopolymerisation of liquid photosensitive polymer solutions facilitated by photoinitiators. This process occurs using visible or ultraviolet (UV) light [26] that can engage with light-sensitive substances, the photoinitiators, inducing the generation of free radicals that start polymerisation [27], resulting in crosslinked hydrogels. Photopolymerisation offers numerous benefits, among them: precise control over polymerisation in terms of both space and time, rapid curing rates at ambient or physiological temperatures, and minimal heat generation [26–28]. Moreover, it presents the capacity to solidify photosensitive polymers, offering the potential to create complex forms that adhere to and match tissue structures [26].

This work compares three different forms of temporary implants: 3D AM scaffolds, hydrogels, and a hybrid strategy combining both previous structures. Mg is used as a promoter for bone regeneration and to improve the mechanical properties of the produced structures.

1.1 Motivation and Objectives

Bone, one of the biggest tissues in our organism, is complex and can recover itself, mechanically and structurally, when slightly damaged. However, in situations of lack of nutrients, mechanical impairment or even defects and traumas of critical sizes, natural healing may not happen, leading to non-union fractures or atypical consolidation. It is also known that Mg is the fourth most abundant element in the human body, being mostly stored in the bone tissue. It plays a pivotal role in the osteoconductive and osteogenic processes. There has been extensive research in bone grafts in recent years, but there is still no viable solution to critical size defects/fractures.

This work aims to develop scaffolds with Mg for bone regeneration to reconstruct critical-size bone defects, considering the applicability to each type and function of bone is distinct, as these structures exhibit unique characteristics among themselves. For such purpose, three main approaches were considered:

1. the manufacture of 3D AM scaffolds combining Mg with a synthetic polymer;
2. the manufacture of photopolymerised hydrogels using a synthetic polymer as a base, incorporated with Mg;
3. the combination of the two previous approaches, 3D AM scaffolds as a structural base and hydrogels with Mg for the delivery of ions, merging the optimal attributes from each individual structure.

The accomplishment of such objectives will undoubtedly contribute to understand the benefits of introducing a biodegradable metal (Mg) in an implant to help bone regeneration, with the addition of being able to characterise and compare results of different forms of bone replacements, offered by TE.

The research work described in this dissertation was carried out following the norms established in the ethics code of Universidade Nova de Lisboa. The work described and the material presented in this dissertation, with the exceptions clearly indicated, constitute original work carried out by the author.

1.2 Structure of the Document

The present document is organised into 5 main chapters.

1. **Introduction**
   An introduction to the theme of the thesis is presented here. This first chapter presents the purpose of the work and its main objectives, intending to describe its contribution to the Biomedical Engineering community and society.
2. **State of Art**
   This chapter presents a general literature review about Mg scaffolds, their advantages

and results in bone regeneration studies. Furthermore, it contains a literature review of the use of an AM technique, Fused Deposition Modelling (FDM), for producing Mg scaffolds and the photopolymerisation technique for producing Mg hydrogels.

3. **Materials and Methods**
   The third chapter describes the materials and methods used to produce the composites used for 3D AM scaffolds, hydrogels, and hybrid strategy. Also, the procedure for the different characterisation techniques is described.

4. **Results and Discussion**
   In this chapter, it is presented the results of the characterisation of the three comparative strategies used. It also presents a discussion about the predicted and the obtained results.

5. **Conclusions and Future Perspectives**
   This final chapter summarises the work carried out. Moreover, recommendations and suggestions are presented for future works, as well as possible improvements to the presented work.

2

State of Art

Bones have the remarkable ability to regenerate their structure and mechanical function, as mentioned earlier, a process that involves intricate complexities. However, the natural restoration process might be hindered under critical conditions such as severe bone defects, insufficient nutrient supply, or compromised mechanical stability, resulting in atypical healing or non-union fractures [8].

The natural regenerative process of bone can be categorized into several phases. The first one involves the inflammatory response, where blood clotting and inflammation set the stage for healing. Subsequently, the reparative phase starts, marked by the formation of a soft callus, followed by the development of a hard callus. This phase ultimately leads to the restoration of bone structure. This process can take only a few months, but it can extend to several years, depending on the type of bone and fracture [29, 30].

Moreover, the hierarchical structure of bone contributes significantly to its mechanical expertise. It exhibits impressive properties essential for its diverse functions. At the macroscopic level, compact bone, with its low porosity (10%), offers strength, while spongy bone, with higher porosity (50 to 90%), contributes to flexibility. The complex interaction among minerals, collagen, and cells within bone results in a material that is both strong and adaptive. The compressive modulus of bone, a measure of its resistance to compression, is a crucial mechanical parameter. These values can range from a few decimals of GPa to 2 GPa for trabecular bone and from 12 to 17 GPa for compact bone [31, 32]. Additionally, bone demonstrates remarkable resistance, a quality vital for its role in providing structural support and protection.

An ideal bone substitute should possess several key characteristics, such as a suitable degradation rate, the ability to promote bone formation (osteogenic), encourage the growth of bone tissue on its surface (osteoconductive), trigger bone-inducing signals (osteoinductive), maintain biomechanical stability, mirror the mechanical properties of the original bone, and exhibit a highly porous structure with interconnected pores [19].

Artificial bone replacements can be produced using biocompatible metals, ceramics, polymers, or combinations of these materials [4]. Metallic biomaterials have gained

extensive use in creating bone replacements, primarily due to their superior mechanical attributes compared to other material categories. Nonetheless, these characteristics occasionally surpass those of natural bone to an extent that can lead to the resorption of surrounding bone tissue post-implantation. To address this concern, adjusting the porosity of these biomaterials becomes crucial. Enhancing porosity can mitigate their mechanical properties while enhancing their capacity to interact with cells and nutrients. This adjustment supports processes like angiogenesis and the integration of new bone tissue [4]. The material surfaces must also exhibit osteoconductive qualities, facilitating cell adhesion, proliferation, and differentiation. Furthermore, the byproducts generated upon materials' degradation must be released appropriately to ensure compatibility with the human body's tolerance levels [4].

In this context, Mg emerges as a promising metal for bone regeneration due to its favourable blend of mechanical and biological properties, particularly its capacity to degrade naturally [19]. Additionally, research indicates that Mg not only contributes to bone strength but also fosters bone growth within the body [33].

2.1 Magnesium forms used in Biomedical Applications

Mg can be used in diverse forms: *i)* a ceramic - magnesium oxide (MgO); *ii)* an inorganic compound - magnesium hydroxide ($Mg(OH)_2$); or *iii)* a salt - magnesium sulphate ($MgSO_4$).

MgO and $MgSO_4$ exhibit a notable difference from $Mg(OH)_2$ as they do not produce hydrogen gas within the body [15]. Furthermore, both are non-toxic, and MgO has demonstrated potential as an anti-biofilm agent which can remove multidrug-resistant bacteria biofilm by inhibiting adhesion and biofilm formation [34], while $MgSO_4$ has been linked to promoting osteogenic activity [35].

While possessing advantages, Mg comes with constraints for medical use when employed alone, primarily due to its rapid corrosion rate. This challenge swiftly diminishes the scaffold's mechanical resilience, impeding the healing of adjacent tissues. To address this concern, the corrosion rate can be enhanced by surface modifications or by combining it with other materials [12].

Numerous investigations have been conducted using MgO, and each study has consistently demonstrated elevated proliferation, adhesion, and differentiation of osteoblast cells. Furthermore, the introduction of nanoparticles led to heightened cell viabilities, along with controlled release of Mg^{2+} ions. This synergistic effect contributed to increased bone volume, promoted angiogenesis, and facilitated the recuperation of critical-size defects [15, 16]. $Mg(OH)_2$, an alternative Mg variant for potential biomedical use, yields a similar reaction product as MgO, differing only in the release of hydrogen gas, which occurs in hydroxide form rather than oxide form [15]. However, despite this drawback, $Mg(OH)_2$, the nanoparticles derived from $Mg(OH)_2$ exhibit promising traits for bone regeneration, stemming from their osteoinductive impact and anti-inflammatory properties.

Additionally, these nanoparticles have been engineered as inorganic antibacterial agents, characterised by strong stability, cost-effectiveness, and antibacterial efficacy [16].

Abdal et al. [9] melded $Mg(OH)_2$ nanoparticles with polymers and indicated that the integration of nanoparticles did not exhibit any cytotoxic effects *in vitro*. Additionally, Park et al. [36] concluded that composite scaffolds displayed improved osteoblastic activity alongside a controlled degradation pattern. In sum, the scaffold's mechanical characteristics were enhanced through the inclusion of these nanoparticles.

In addition to the aforementioned Mg forms, $MgSO_4$ also emerges as a viable form for utilising this metal in the context of bone regeneration. Chen et al. [37] noted that incorporating $MgSO_4$ heptahydrate into calcium sulphate can transform its crystal structure, leading to the formation of cubic crystals. This alteration, when combined with the introduction of bioglass, boosts the composite's mechanical properties. The utilisation of $MgSO_4$ further fosters osteogenic activity, stimulating osteoblast differentiation and facilitating bone formation, which is integral for maintaining bone resistance and density. Additionally, the release of Mg ions could potentially support the development of mesenchymal stem cells.

2.2 Magnesium Scaffolds

The inclusion of Mg in scaffolds for bone regeneration has yielded significant enhancements, as widely recognised.

A porous scaffold composed of 70% Mg powder, combined with sodium chloride particles and ethanol as a binder, was fabricated. The scaffold's corrosion behaviour was assessed by quantifying the release of hydrogen gas during the corrosion process. Coating layers of hydroxyapatite (HA) were applied. Scaffolds with 70% porosity were successfully manufactured, exhibiting no observable cracks or defects. The pore sizes ranged between 200 and 400 μm, and the pores were evenly distributed and interconnected. A noteworthy outcome was the corrosion suppression achieved by the coating layers. However, these coatings limits the strength of the scaffold, a limitation for their use in load-bearing orthopaedic applications [11].

Abdal-hay et al. [9] employed bioresorbable $Mg(OH)_2$ nanoparticles at 5 and 20 wt% in combination with PCL to regulate degradation and enhance mechanical properties and bioactivity. The resulting scaffolds exhibited interconnected, open pores that positively influenced cell growth rate and cellular migration. The addition of just 5 wt% of nanoparticles resulted in enhancements in scaffold tensile properties. In contrast, the addition of 20 wt% accelerated the degradation rate, particularly under immersion in PBS (Phosphate-buffered saline, a solution used in biological research containing water and salts). The study's outcomes imply that employing 5 wt% of $Mg(OH)_2$ nanoparticles could be advantageous for bone applications requiring long-lasting mechanical integrity, such as osteoporotic fractures. Meanwhile, 20 wt% of nanoparticles could be applied to

situations where enhanced bioactivity is crucial, while mechanical properties play a lesser role — like in bone fillings or dental bone grafts [9].

Mg was also incorporated with Poly(lactic-co-glycolic acid), PLGA, at 5 and 15 wt%. The PLGA/$Mg(OH)_2$ scaffold exhibited lower cell death than the control scaffold (PLGA only). Consequently, it was proposed that the nanoparticles might inhibit calcification, implying that a synthetic polymer scaffold containing $Mg(OH)_2$ could promote cartilage regeneration and offer potential benefits in the care of orthopaedic patients [36].

An additional investigation involved the utilisation of four sets of scaffolds: *i)* PCL; *ii)* PCL with 5 wt% Mg; *iii)* PCL with 10 wt% Mg; and *iv)* PCL with 15 wt% Mg. This study aimed to assess whether the inclusion of Mg powder enhances the scaffold's porous architecture and influences the biocompatibility of PCL. The PCL/Mg scaffolds displayed a notably rougher surface, a positive enhancement as cells tend to favour rougher surfaces over smoother ones. The study proposed that 10 wt% Mg might influence bone remodelling during defect repair. Furthermore, superior cell adhesion and growth outcomes were observed in the 5 wt% and 10 wt% groups compared to both PCL and 15 wt% groups. Subsequent testing indicated that the gradual release of Mg ions and pH levels within the 10 wt% group exhibited a more moderate pattern compared to the other groups. Consequently, the scaffolds with 10 wt% Mg demonstrated the most favourable outcomes, resulting in increased bone formation and reduced overall healing time, thus showcasing their potential as materials for orthopaedic applications [7].

MgO has also been combined with PCL using 3D printing, specifically through an extrusion-based low-temperature approach. The resulting scaffolds displayed interconnectivity and well-defined pores. Studies involving the *in vivo* implantation of femoral components and the treatment of critical-sized cranial bone defects revealed that, after an 8-week period of implantation, scaffolds released Mg^{2+} ions exhibiting noteworthy increases in bone volume, improved angiogenesis, and near-complete recovery of the critical-sized defect [15]. Furthermore, scaffolds comprised of Mg and coated with fluorohydroxyapatite (FHA) revealed that surface modification of the Mg-based scaffolds reduced the degradation rate, maintained mechanical strength, and provided favourable surface biocompatibility. Moreover, cell culture on these scaffolds showed great proliferation [38].

2.3 Magnesium Hydrogels

In recent years, hydrogels have emerged as a versatile and promising class of materials with a wide range of applications in biomedicine. These 3D networks, composed of water-swollen polymers, possess a remarkable ability to mimic the natural environment of living tissues. This unique characteristic has propelled hydrogels into the forefront of biomedical research, offering innovative solutions for drug delivery and TE.

These materials, characterised by their high-water content and exceptional biomimetic qualities, are similar to the ECM and have particular appeal as 3D environments for cell

culture and delivery systems. Hydrogels predominantly rely on diffusion to transport oxygen, nutrients, and waste materials. Incorporating cells within hydrogels provides a straightforward means of injection into targeted regions, thereby avoiding additional open surgeries. This approach is especially advantageous for patients with irregular, deep or enclosed defects [10].

In a study by Yin et al. [14], they developed an ionic crosslinked hydrogel using Mg^{2+}-alginate. The outcomes revealed an enhanced attachment of osteoblasts with the incorporation of Mg. Intriguingly, as the Mg^{2+} content increased, there was a simultaneous reduction in sodium ions (Na^{+}), implying an ion exchange phenomenon within the gel. Additionally, an escalation in gel density corresponding to higher Mg^{2+} concentrations and a rise in the compressive modulus were observed. Furthermore, the hydrogel's swelling ratio decreased in the presence of Mg, indicating modifications in the microstructure that positively impacted both protein adsorption and cell incorporation [14].

The findings of Tang et al. [10] indicated that the degradation of Mg resulted in the generation of Mg^{2+} ions, which promoted osteogenic differentiation of stem cells and facilitated bone regeneration. Additionally, the augmentation of nanoparticles led to a decrease in the elastic modulus due to the higher porosity within the hydrogels. It's worth noting that no indications of cytotoxicity were observed in their study [10].

As previously documented in research, Mg has shown potential for boosting bone regeneration. However, these earlier studies predominantly focused on a single type of Mg. In our study, we conducted a comparative analysis between two distinct forms of Mg to assess their influence on temporary implants' mechanical and chemical properties. As rarely seen in other works, we also pursued a combination of two distinct structural approaches commonly employed in bone regeneration: 3D AM scaffolds and hydrogels. This fusion aims to bind the most favourable traits from each individual structure, enhancing the overall effectiveness of the approach.

3

Materials and Methods

3.1 Manufacturing

3.1.1 Three-Dimensional Additive Manufactured temporary implant

The base polymer of choice was Poly(ϵ-caprolactone), with a molecular weight of 6500 g/mol. For magnesium sources, commercially obtained magnesium oxide (97%, MERCK) and magnesium sulphate (99.5%, MERCK) were employed.

Using the solvent-casting (SC) technique, composites were fabricated by blending PCL with MgO and $MgSO_4$, utilising chloroform ($CHCl_3$) (Fisher Chemical) as the organic solvent. Various compositions were prepared as shown in Table 3.1: *i)* pure PCL, serving as a control sample; *ii)* PCL with 5% MgO; *iii)* PCL with 10% MgO; *iv)* PCL with 15% MgO; *v)* PCL with 5% $MgSO_4$; *vi)* PCL with 10% $MgSO_4$; and *vii)* PCL with 15% $MgSO_4$.

Table 3.1: Biomaterials mixtures produced using different forms and percentages of Mg (magnesium oxide, MgO; and magnesium sulphate, $MgSO_4$).

Base-Polymer	***Form of Mg***	***Percentage of Mg (wt%)***	***Nomenclature***
PCL	-	-	PCL
	MgO	5	5% MgO
		10	10% MgO
		15	15% MgO
	$MgSO_4$	5	5% $MgSO_4$
		10	10% $MgSO_4$
		15	15% $MgSO_4$

For the preparation of these composites, firstly, a PCL-based solution was made using a PCL:$CHCl_3$ (1:3) (w/v) ratio, containing 40 g of PCL and 120 mL of $CHCl_3$. It was prepared under constant stirring (250 rpm) and, subsequently, the predetermined forms and concentrations (2, 4 and 7 g of Mg, for 5, 10 and 15%, respectively) of Mg were introduced and continuously stirred until complete dispersion. Solutions were then deposited into Petri dishes and goblets at room temperature (RT), allowing the complete solvent evaporation and subsequent drying of the mixture. Lastly, after a 7-day period, composite membranes and cylindrical discs resulting from the evaporation of the mixture in the Petri dishes and goblets were successfully acquired.

For the manufacture of the scaffolds using 3D printing technique, an equipment developed at the Centre for Rapid and Sustainable Product Development of the Polytechnic of Leiria (Leiria, Portugal), called Bioextruder [39] was used. Before initiating the printing of the structures, it was necessary to cut the previously manufactured membranes into small pieces resembling pellets.

The scaffolds were designed to exhibit a circular cross-section measuring 10 mm in diameter and 3 mm in height and filament and pore diameters of about 300 μm. Each scaffold comprised 10 layers, each rotated by 90° in relation to the previous one, resulting in a lay-down pattern of 0°/90°. Hence, a nozzle of 0.4 mm was employed alongside with a melting temperature of 90°C.

3.1.2 Hydrogel-based temporary implant

Hydrogels were created using a synthetic polymer base, PEGDA average 575 Mn (Sigma-Aldrich®), with the inclusion of 2.5% (w/v) magnesium sulphate (99.5% $MgSO_4$, MERCK), as indicated in Table 3.2. $MgSO_4$ was used because it is a salt, which signifies that it is is more easily dissolved in PEGDA. Moreover, this type of Mg achieved a higher compression modulus in the scaffolds in both 5% and 15% wt groups, compared to the MgO groups. The percentage of 2.5% wt of $MgSO_4$ was used not only because it is a value close to the 5% used in the scaffolds (percentage with better results) but also because it is known that the weight percentage of Mg in bones is between 1% and 2% (these values also depend on factors such as gender, age, health, etc.) [40].

Table 3.2: Hydrogels' preparation with a synthetic base-polymer.

Base-Polymer	***$MgSO_4$ content (w/v)***	***Nomenclature***
Polyethyleneglycol diacrylate, PEGDA	-	PEGDA
	2.5%	PEGDA:Mg

For the hydrogel preparation, a mixture of 0.1% (w/v) IRGACURE 651 photoinitiator (BASF) was blended with PEGDA and stirred for 10 minutes at 340 rpm. Additionally, a solution of 5% (w/v) $MgSO_4$ was simultaneously dissolved in distilled water (dH_2O) for 10 minutes at 340 rpm. Subsequently, the two mixtures were combined in a 1:1 ratio and stirred for 25 minutes at 340 rpm. PEGDA hydrogels served as a control. Ultimately, these mixtures were placed into cubic moulds and subjected to curing with 365 nm UV light for 8 minutes.

3.1.3 The hybrid strategy for temporary implant

A hybrid strategy was also made, combining the two previous forms of temporary implant, the 3D additive manufactured scaffolds and the hydrogels incorporated with Mg. The PCL scaffold was used as the main structure of the implant, while the hydrogel was incorporated with $MgSO_4$ and used as a delivery vehicle for bioactive ions to promote bone regeneration.

Both scaffolds and hydrogels were made using the method mentioned above. The only difference in the procedure was that the scaffolds were placed in cubic moulds, and the hydrogel mixture was injected, with the help of a syringe, before its cure with the UV light.

3.2 Physicochemical Characterisation

3.2.1 Morphological characterisation

The pore and filament diameters of the produced 3D AM temporary implant scaffolds were examined using an optical microscope (Leica DM750M Microsystems, Northbrook, IL, USA) at a magnification of 50x.

Scanning Electron Microscopy (SEM) combined with Energy-Dispersive X-ray Spectroscopy (EDS) technique was used to provide insights into the surface morphology and elemental composition and distribution of the various specimens in the 3D AM scaffold, using a Tabletop microscope TM3030 Plus Hitachi equipment, with magnifications of 50x and 200x. The samples were fixed on the sample holder disk using a conductive carbon tape and coated with a thin layer of Au-Pd.

3.2.2 Chemical Composition of 3D additive manufactured temporary implant

Fourier Transform Infrared Spectroscopy (FTIR) technique was performed to assess the chemical composition, the presence of specific functional groups and the molecular structure of the scaffolds in a PerkinElmer Spectrum IR Version 10.7.2 spectrometer.

3.2.3 Crystallography of 3D additive manufactured temporary implant

The X-ray Diffraction (XRD) was performed on 5 samples using a PANalytical Xpert PRO MRD equipment diffractometer. Difractograms were recorded with a Cu/Kα irradiations(λ = 1.540598 Å), and 2-theta range of 10 to 60 was used to evaluate and study the crystal structure and phase composition of the 3D AM temporary implant.

3.2.4 Mechanical Performance to compression

An INSTRON 5584 equipment (50 tons) was used to assess the mechanical performance of the row material composites (discs resulting from the goblet evaporation of the SC mixtures) and the porous materials (scaffolds) when submitted to compressive stress and for the hybrid strategy (N = 5). Two different extension rates were used: 2 mm/min for the discs and 1 mm/min for the scaffolds and the hybrid strategy. The compressive Young's Modulus was determined by the slope of the linear portion of the stress-strain curve, which corresponds to the material's elastic region.

A Texture Analyser equipment (TA.XT.plusC) was employed to assess the mechanical response of the hydrogels under compression (N = 5), providing deeper insights into their behaviour when exposed to compressive stresses. The testing was carried out at an extension rate of 1.2 mm/min and a cell load of 50 kg. Compressive Young's Modulus was calculated in the same way as for the 3D AM temporary implant.

3.2.5 Degradation performance of hydrogels

Hydrolytic degradation tests were carried out on the hydrogels to evaluate their response (measured by mass loss) in a hydrated environment, simulating the native conditions over a designated time frame. Samples were tested for a period of 5 weeks (N = 3). The process began with weight measurement on day 0 to establish the initial mass, as a dry hydrogel. Subsequently, a new weighing, following removing the water previously placed, was conducted after 24 hours. Afterwards, assessments were performed twice a week throughout the test duration.

3.3 Statistical Analysis

GraphPad Prism© software version 10.0.3 was used for statistical analysis. The statistical significance level was established at a confidence level of 95%. Results of significance were considered as: *P<0.05,**P<0.01, and ***P<0.001.

4

Results and Discussion

4.1 3D Additive Manufactured Temporary Implant

By employing the technique of SC, composites made of PCL and 2 different forms of Mg, MgO and $MgSO_4$, were prepared. Cylinders of PCL and PCL with different percentages of MgO and $MgSO_4$ (5, 10 and 15%), ideally non-porous, were produced with 33 mm and 6 mm of diameter and height, respectively (Figure 4.1). Figure 4.1a shows the top and side views of a homogeneous disc. Since the evaporation of the organic solvent (chloroform) used during scaffold preparation with SC methodology is not easily controlled, some of the obtained discs showed undesired porosity, with multiple macro pores in the different samples. Figure 4.1b shows the side views of heterogeneous discs, showing discrepancies in their morphologies, presenting some macro pores resulting from the organic solvent's uncontrolled evaporation.

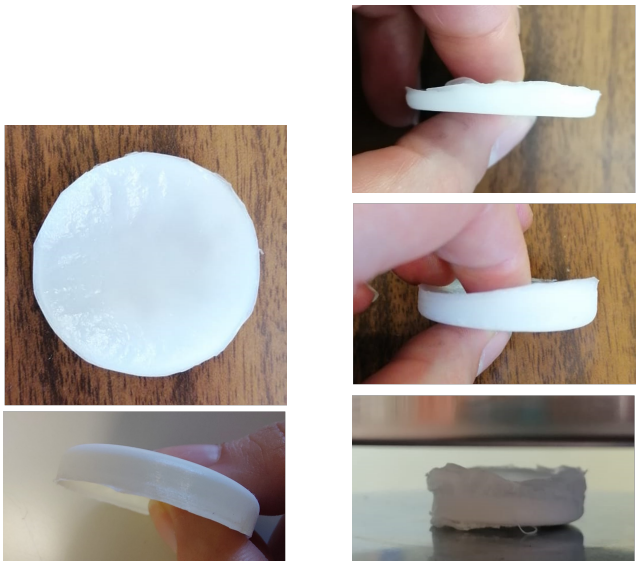

(a) (b)

Figure 4.1: Discs overall morphology: (a) top and side views of a homogeneous disc; and (b) side views of heterogeneous discs.

Results revealed that the introduction of both forms of Mg leads to a decrease in ductility when compared with the control group. However, while the ductility decreases with the increase of MgO content, the opposite behaviour occurs with $MgSO_4$, where ductility increases with the increase of $MgSO_4$ content. Concerning the strength evaluated through the compressive Young's Modulus (Appendix A.1), the incorporation of 5% Mg increased the modulus (from 96.0±26.0 MPa to 133±47.0 MPa in MgO and 157±4.00 in $MgSO_4$), while the increase of Mg content to 10% lead to a slight decrease of the Young's Modulus value to 92.0±13.0 MPa in MgO and 91.0±9.00 MPa in $MgSO_4$, when compared with the control group. In MgO, the introduction of 15% slightly increased the modulus compared to 10%, while in the $MgSO_4$, the modulus slightly decreased compared to 10% content. These discrepancies can be explained by the presence of macro pores in the discs, which negatively affects the reproducibility of the outcomes. Results are summarised in Figure 4.2.

Since the evaporation of the organic solvent (chloroform) used during scaffold preparation with SC methodology is not easily controlled, the obtained discs showed some undesired porosity, with the presence of multiples macro pores in the different samples. The stress-strain curves are showed in Figure 4.2, as well as the Young's Modulus of each group.

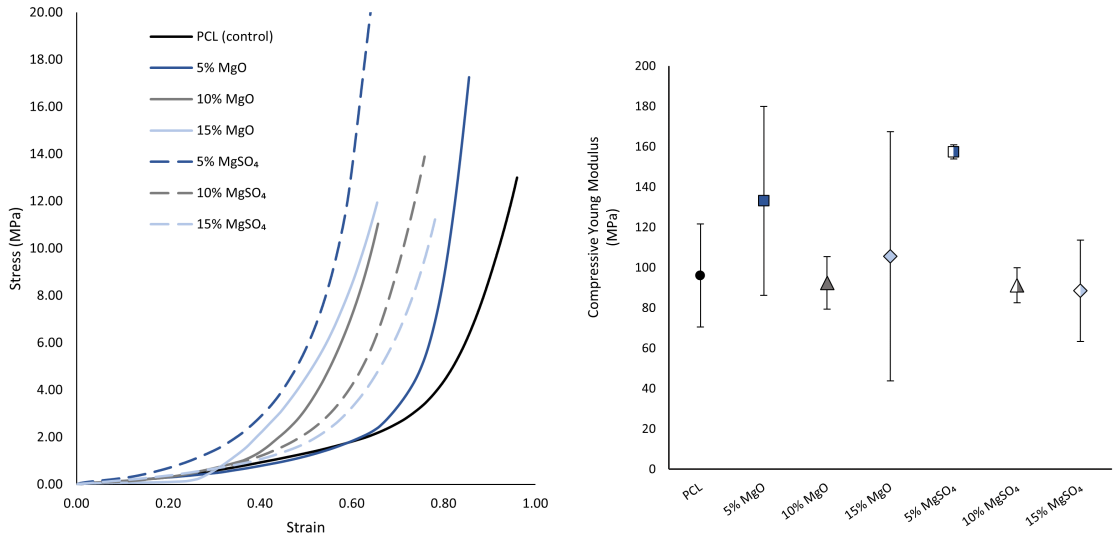

(a) (b)

Figure 4.2: Mechanical performance of discs to compression (N = 3): (a) stress-strain curves and (b) compressive Young's Modulus.

3D AM scaffolds combining PCL and Mg were successfully created through AM technology. Initial visual assessment allowed the identification of distinctions between the PCL and two Mg forms (Figure 4.3). Notably, scaffolds containing MgO (Figure 4.3b and Figure 4.3c) exhibited a more pronounced yellowish hue than those with $MgSO_4$ (Figures 4.3d and 4.3e). This contrast was particularly evident with the scaffolds containing a higher content of MgO (15% MgO) (Figure 4.3c).

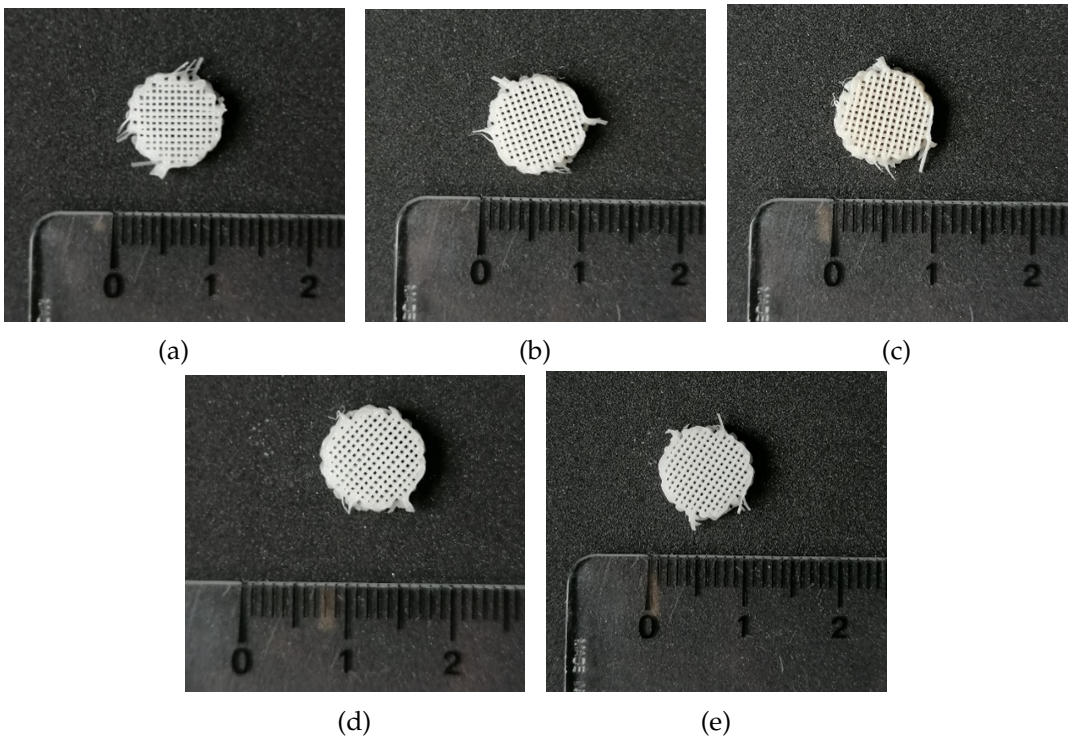

Figure 4.3: 3D additive manufactured scaffolds of: (a) PCL; and scaffolds of PCL with (b) 5% MgO, (c) 15% MgO, (d) 5% $MgSO_4$, and (e) 15% $MgSO_4$. Scale is in centimetres.

As mentioned earlier, both filament and pore sizes were designed to be 300 μm. This value was set since studies in the literature refer this to be within the ideal size for bone tissue regeneration [2, 17]. However, morphological examination of the manufactured scaffolds using optical microscopy exposed slight deviations from the theoretical values (Table 4.1). Notably, among scaffold types, the 5% MgO scaffolds demonstrated a closer alignment with the intended filament diameter (301±11.0 μm), while the 15% $MgSO_4$ scaffolds exhibited a more accurate pore size (287±5.00 μm). Interestingly, there's an observable trend of filament diameter increase with rising Mg content in the case of MgO, reaching 310±10.0 μm. Conversely, a contrasting pattern is evident for $MgSO_4$, where the diameter experiences a reduction of approximately ~16% (decreasing from 311±15.0 μm to 263±11.0 μm). As for pore size, an inverse relationship with Mg concentration is evident in both scenarios. The PCL and 5% MgO scaffold recorded the most substantial values, exceeding the predetermined value by roughly ~15%.

For effective cell attachment to the scaffold, pores must strike a balance: they should be sufficiently large to facilitate the diffusion of nutrients and oxygen yet small enough for cells to interact with the 3D environment and adhere to the scaffold [2]. The findings from this study align well with the requirements for successful bone regeneration and are consistent with existing literature since it was set that pore sizes between 70 and 400 μm significantly contribute to bone growth, formation of new tissue, and vascularisation [2, 17, 41].

Table 4.1: Morphological analysis of 3D scaffolds for the different groups of samples: PCL and PCL with different Mg content with average filament and pore size values (N = 7). Scale bar is 50 μm.

Group	*Microscopy (50x)*	*Filament (μm)*	*Pore (μm)*
PCL	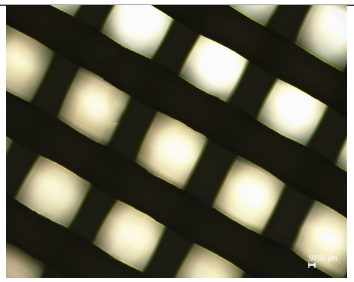	279±12.0	346±25.0
5% MgO	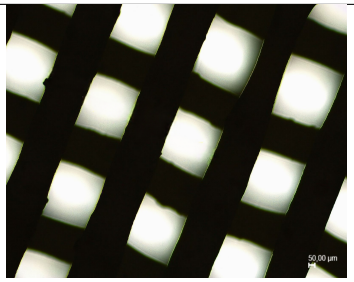	301±11.0	350±10.0
15% MgO	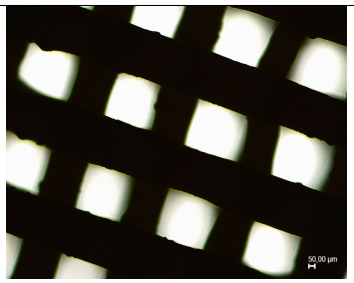	310±10.0	320±11.0
5% $MgSO_4$	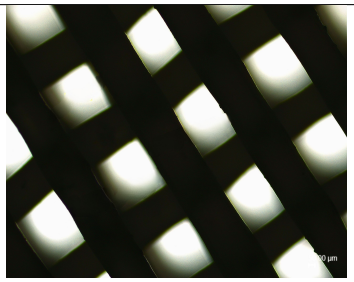	311±15.0	327±32.0
15% $MgSO_4$	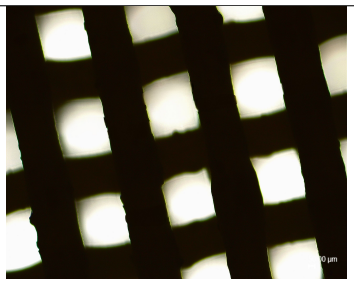	263±11.0	287±5.00

The assessment of the scaffolds' mechanical properties served a dual purpose: to identify the optimal form of Mg for bone TE applications and to determine the ideal Mg content. Existing literature cites the utilisation of $Mg(OH)_2$ at approximately 5% to 20% [9] and Mg powder at 5%, 10%, and 15% [7]. Notably, 5% is recommended for scenarios prioritising mechanical attributes, while 20% is suggested to enhance biological activity due to its inherent bioactivity [9].

Furthermore, the importance of Mg ions in promoting osteoblast proliferation and their affinity for hydroxyapatite in bones to prevent bone loss and fragility is acknowledged. However, excessive concentrations can have counterproductive effects. Consequently, scaffolds were manufactured within the explored range, yielding positive outcomes (at 5% and 15% concentrations) but employing other Mg forms.

Results from compressive tests are presented in Figure 4.4. Analysis of the curves confirms that the inclusion of Mg in the thermoplastic material positively impacts the scaffold's performance in terms of resistance compared to the control. As expected, results confirm that introducing a ceramic material (MgO) increases resistance while reducing ductility. Another contributing factor that aligns with and reinforces this observation is the enlargement of filament diameter, coupled with a reduction in pore size, indicative of decreased overall scaffold porosity. Interestingly, despite the strength increase, Young's Modulus for compression (Appendix A.2) decreases by around 32% (from 282±41.0 MPa to 193±31.0 MPa). This reduction can be attributed to the high magnesium content, which prompts the formation of particle agglomerates, introducing more areas of fragility within the scaffolds [9]. Concerning the $MgSO_4$ scaffolds, the graphs exhibit notable similarity, indicating minimal variations. Even so, a significant decline in Young's Modulus is evident, diminishing from 291±25.0 to 233±31.0 MPa, marking a decrease of nearly 20%. The SEM images of the compressed scaffolds can be visualised in Appendix B.1.

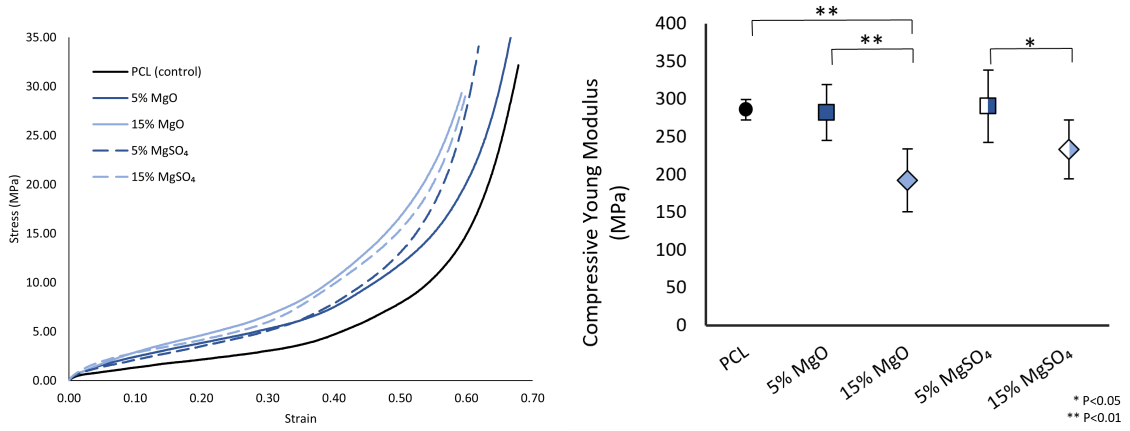

(a) (b)

Figure 4.4: Mechanical performance of scaffolds to compression (N = 5): (a) stress-strain curves and (b) compressive Young's Modulus. One-way ANOVA was performed, and statistical differences are presented as: (*) P<0.05 and (**) P<0.01.

SEM images were obtained for both compressed and not compressed scaffolds. EDS was also employed to visualise the distribution of the elemental compounds in the scaffolds. Results are shown in Table 4.2.

Table 4.2: SEM and SEM/EDS images of the produced scaffolds: PCL, 5% MgO, 15% MgO, 5% $MgSO_4$ and 15% $MgSO_4$. Top view is presented.

Group	*Top view SEM images (200x)*	*Carbon (C), EDS image (200x)*	*Oxygen (O), EDS image (200x)*	*Magnesium (Mg), EDS image (200x)*	*Sulfur (S), EDS image (200x)*
PCL	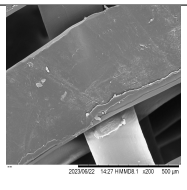	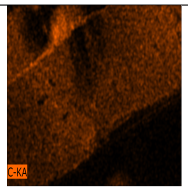	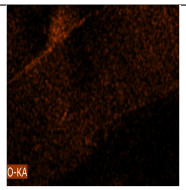		
5% MgO	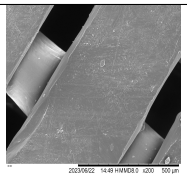	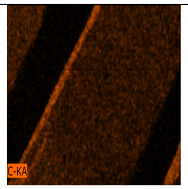	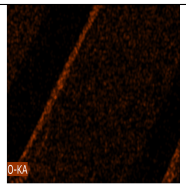	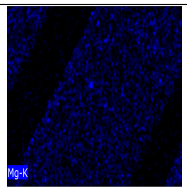	
15% MgO	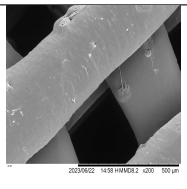	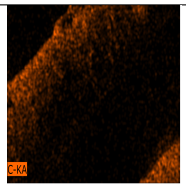	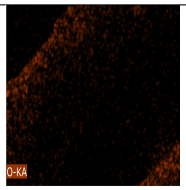	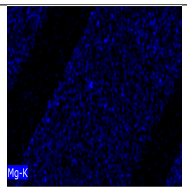	
5% $MgSO_4$	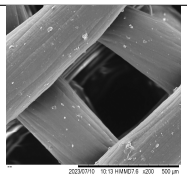	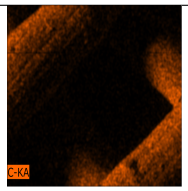	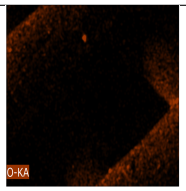	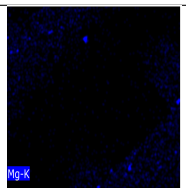	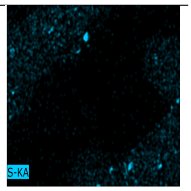
15% $MgSO_4$	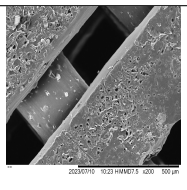	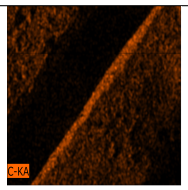	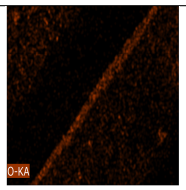	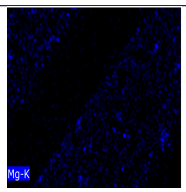	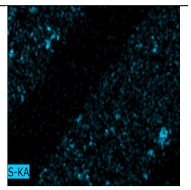

The introduction of Mg made the surface rougher than the control group. The incorporation of $MgSO_4$ made this change more noticeable, especially with the highest content of Mg (15% $MgSO_4$), which can actually become more prominent due to the presence of the sulfur element. This alteration can positively affect cell adhesion once the cells prefer irregular surfaces to smooth ones [7, 9]. The elements Carbon (C) and Oxygen (O) are consistently found in all groups of scaffolds, primarily due to the chemical composition of PCL, which includes both elements in its structure. Mg particles were

scattered randomly over the surface of the scaffold, confirming a uniform distribution of Mg within the polymer matrix. Furthermore, the element sulfur (S) is observed in the groups containing $MgSO_4$, owing to its presence in the chemical composition of this type of Mg.

XRD analysis was performed to evaluate the phase composition of the produced scaffolds, presented in Figure 4.5. PCL curve presented typical peaks at 21.3° and 23.8°, associated with the (110) and (200) crystallographic planes, respectively [42, 43]. A peak at 36.1° is also observed, but no literature describes it as a typical peak of PCL structure. The characteristic peaks of MgO at 37° (111 reflection) and 42.8° (200 reflection) are observable in the two diffractometric profiles, even though the 37° peak can be scarcely observed due to its very low intensity [16, 44]. We can also see that increased MgO content enhanced the 42.8° peak. No diffraction peaks of $MgSO_4$ are discernible in the examined PCL/$MgSO_4$ samples, signifying that this type of Mg has minimal impact on the crystal structure of the PCL matrix and does not markedly influence the XRD patterns.

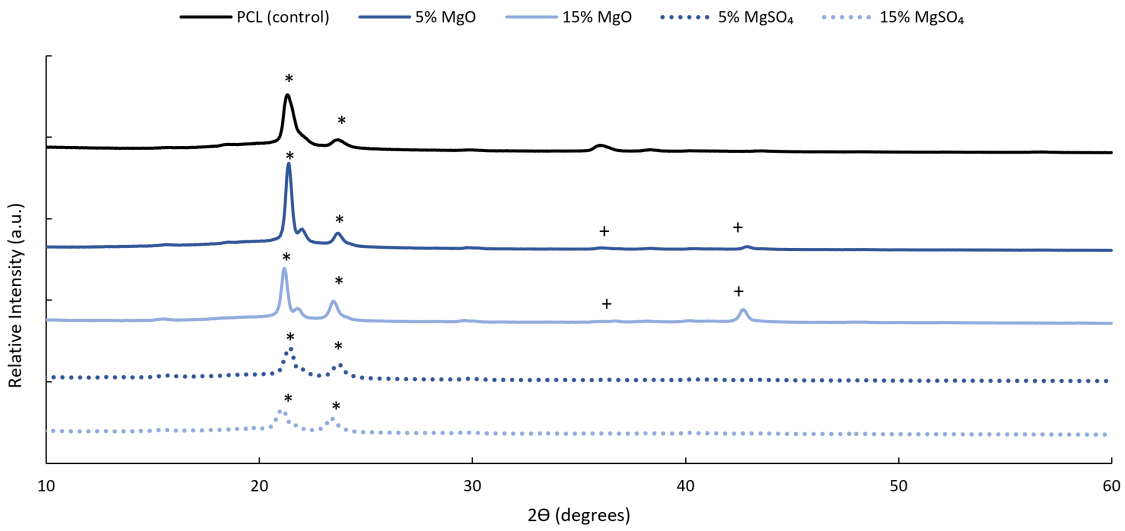

Figure 4.5: Phase composition (XRD) of the different groups of the scaffolds: PCL, 5% MgO, 15% MgO, 5% $MgSO_4$ and 15% $MgSO_4$ - typical peaks (*) for PCL and (+) for MgO.

FTIR analysis was conducted to assess the chemical composition of the manufactured scaffolds, as illustrated in Figure 4.6. PCL exhibits characteristic peaks at approximately 961, 1164, 1240, and 1294 cm^{-1}, corresponding to the C-O bond. Peaks associated with the C-H bond can be observed at 1368, 2867, and 2946 cm^{-1}, and the peak indicates the presence of the carbonyl stretching mode at 1722 cm^{-1}. Additionally, a C-C peak is observed at around 1471 cm^{-1} [42, 45]. All these peaks are observed in all groups because PCL is always present. In the MgO groups, a peak at approximately 732 cm^{-1} signifies the stretching mode of Mg-O-Mg bonds [46], while in the $MgSO_4$ groups, wave numbers at 961 and 1164 cm^{-1} indicate the stretching vibrations of $SO_4{}^{-2}$ [47]. These peaks are hardly distinguishable as they nearly coincide with the PCL peaks.

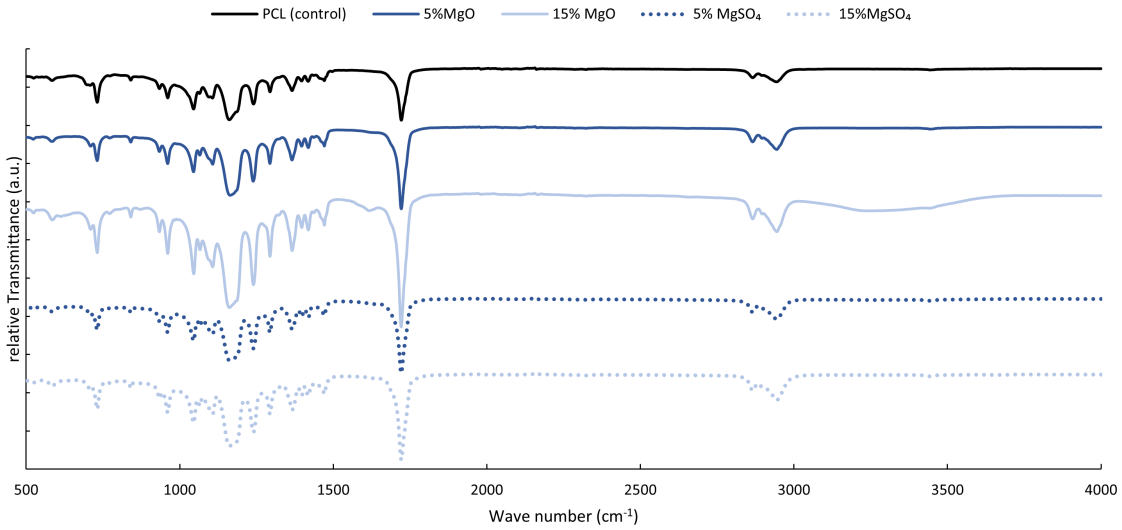

Figure 4.6: Chemical composition through Fourier Transform Infrared Spectroscopy (FTIR) of the different scaffolds: PCL, 5% MgO, 15% MgO, 5% $MgSO_4$ and 15% $MgSO_4$.

4.2 Hydrogel-based Temporary Implant

Another approach was tested with hydrogels instead of 3D AM scaffolds to compare mechanical properties with the incorporation of Mg.

A synthetic polymer (PEGDA) was combined with active Mg ions to create hydrogels successfully. PEGDA was used since it is a photopolymerisable and biocompatible polymer presenting nontoxicity and non-immunogenicity [48, 49].

The resultant hydrogels exhibit approximately 22 x 22 x 3 mm (Figure 4.7). The inclusion of Mg is readily discernible within these hydrogels. Notably, the hydrogel containing Mg (Figure 4.7b) is characterised by a white hue, confirming the presence of Mg, while the counterpart without it remains colourless (Figure 4.7a).

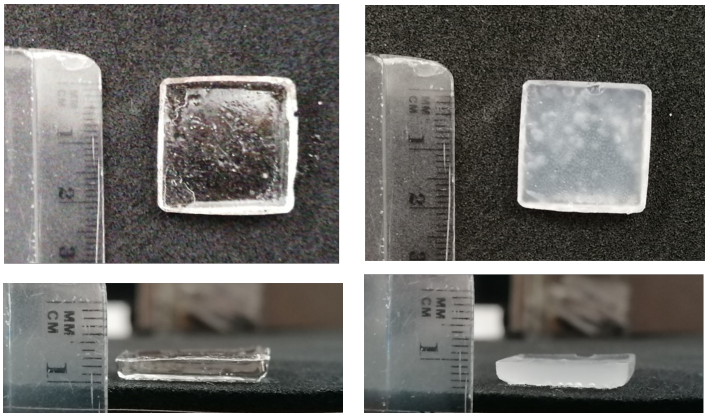

(a) (b)

Figure 4.7: PEGDA-based hydrogels produced (from top and front perspectives): (a) PEGDA; and (b) PEGDA:Mg. Scale is in centimetres.

The mechanical properties of the hydrogels were assessed to gain insight into the impact of Mg incorporation on their mechanical strength. This evaluation aimed to understand how the hydrogels respond to compressive forces primarily experienced by bones.

The outcomes of the compression test are presented in Figure 4.8. Incorporating Mg led to a noteworthy 23% increase in the compressive Young's Modulus (Appendix A.3) of the hydrogels (from 1.85±0.200 MPa to 2.28±0.120 MPa), thereby enhancing their mechanical strength and ability to withstand compression forces (as indicated in Figure 4.8b). A maximum force of 50 kg was applied, and none of the hydrogels reached their breaking point during the test. Furthermore, the ductility of the hydrogels exhibited improvements. A comparison of the heights before and after compression highlighted the elasticity of the samples with Mg incorporation (depicted in Figures 4.8c and 4.8d).

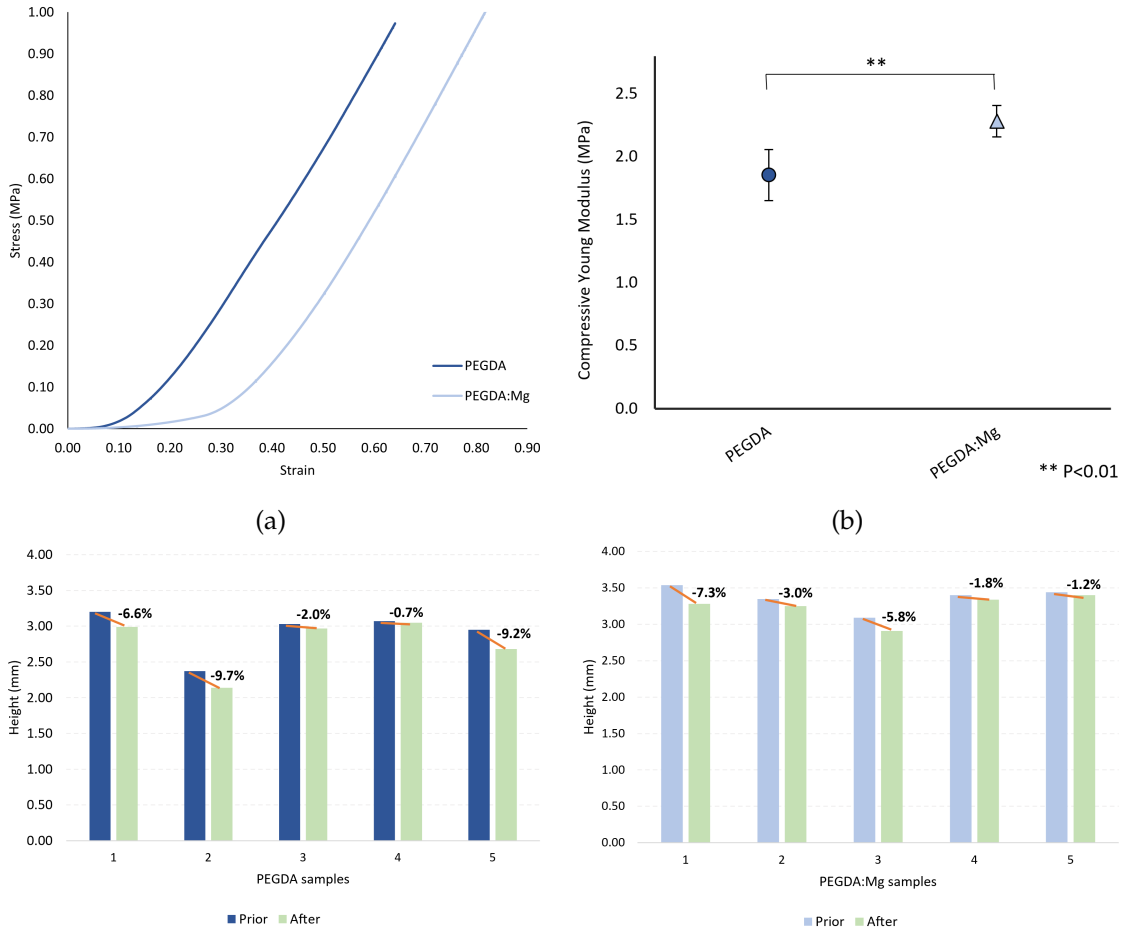

Figure 4.8: Mechanical performance of PEGDA and PEGDA:Mg hydrogels under compression (N = 5): (a) Stress-strain curves; (b) Compressive Young's Modulus; and (c) Difference in height before and after compression. A t-test was conducted, and the resulting statistical disparities are indicated as: **P < 0.01.

Hydrogel degradation under hydrated conditions was performed to evaluate their performance over a specific duration. The outcomes of this study are visualised in Figure 4.9.

The results demonstrate a noticeable initial weight increase in the PEGDA hydrogels during the initial days. This phenomenon is more pronounced than the weight increase observed in the PEGDA:Mg hydrogels. This phenomenon can be explained as PEGDA possesses hydrophilic properties, and the presence of Mg occupies a portion of the hydrogel, Mg limits its ability to absorb the surrounding medium. Subsequently, a plateau is reached, and a gradual decrease in mass occurs. Interestingly, both groups, with and without Mg, exhibit similar behaviour when exposed to a hydrated environment. Both sets of hydrogels demonstrate stability over the one-month experiment duration.

This degradation pattern aligns with the desired degradation characteristics for bone regeneration applications, since in bone healing natural process, three partially overlapping phases occurs - inflammatory, repair and remodelling -, beginning immediately after the fracture or trauma happens [29, 30, 50, 51]. Bone healing can take several months, even years, so the adequate support is needed, from the start to the end of the restoration. Such applications require a controlled, gradual release of bioactive ions to facilitate bone regeneration. Through this prolonged ion release mechanism, the material ensures a continuous supply of necessary elements for promoting bone formation. This controlled release strategy supports the healing process, promotes effective bone regeneration, and prevents the accumulation of potentially harmful ion levels.

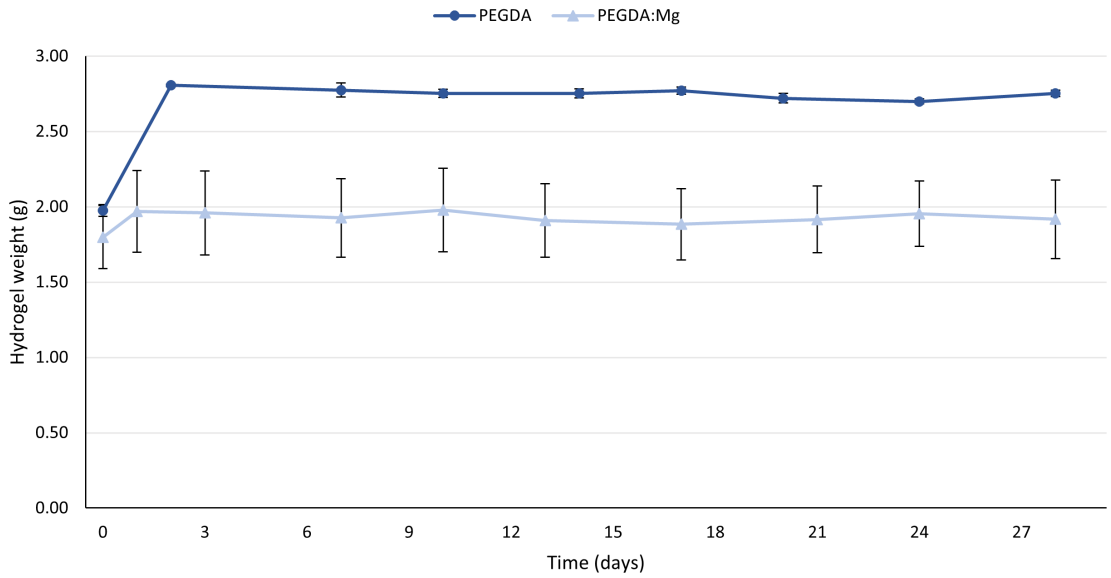

Figure 4.9: Hydrolytic degradation outcomes of both PEGDA and PEGDA:Mg hydrogels. They are summarised in terms of average weight along with the corresponding standard deviation (N = 3).

4.3 The Hybrid Strategy for Temporary Implant

The hybrid strategy, a combination of the 3D AM scaffolds of PCL with a PEGDA:Mg hydrogel, was successfully produced (Figure 4.10).

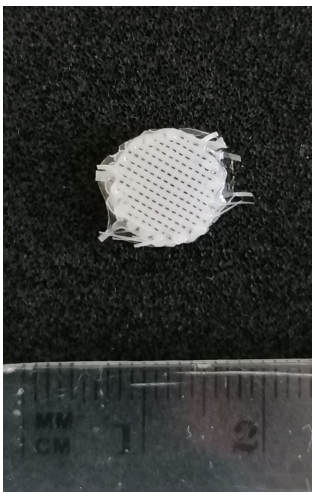

Figure 4.10: Hybrid scaffold – combination of 3D AM scaffolds of PCL with PEGDA:Mg hydrogel. Scale is in centimetres.

This strategy's performance to compression is shown in Figure 4.11, together with the two individual structures, scaffold and hydrogel.

The increase in the compressive Young's Modulus (Appendix A.4) for the hybrid strategy is highly perceptive: an increase of about 567% is observed from the modulus of the scaffold to the modulus of the hybrid strategy (from 286.0±21.00 MPa to 1908±82.00 MPa). So, the hybrid strategy reached a modulus of almost 2 GPa, which fits with the theoretical values of the natural bone, extending from a few decimal of GPa to 2 GPa for trabecular bone and ranging from 12 to 17 GPa for compact bone [31, 32]. There is also a decrease in ductility and an increase in resistance of the hybrid strategy compared to the two individual structures. These results demonstrate an enhancement in the mechanical properties when combining the two individual structures into a single entity. Next steps should involve cell culture studies to the hybrid structures to verify the biological behaviour.

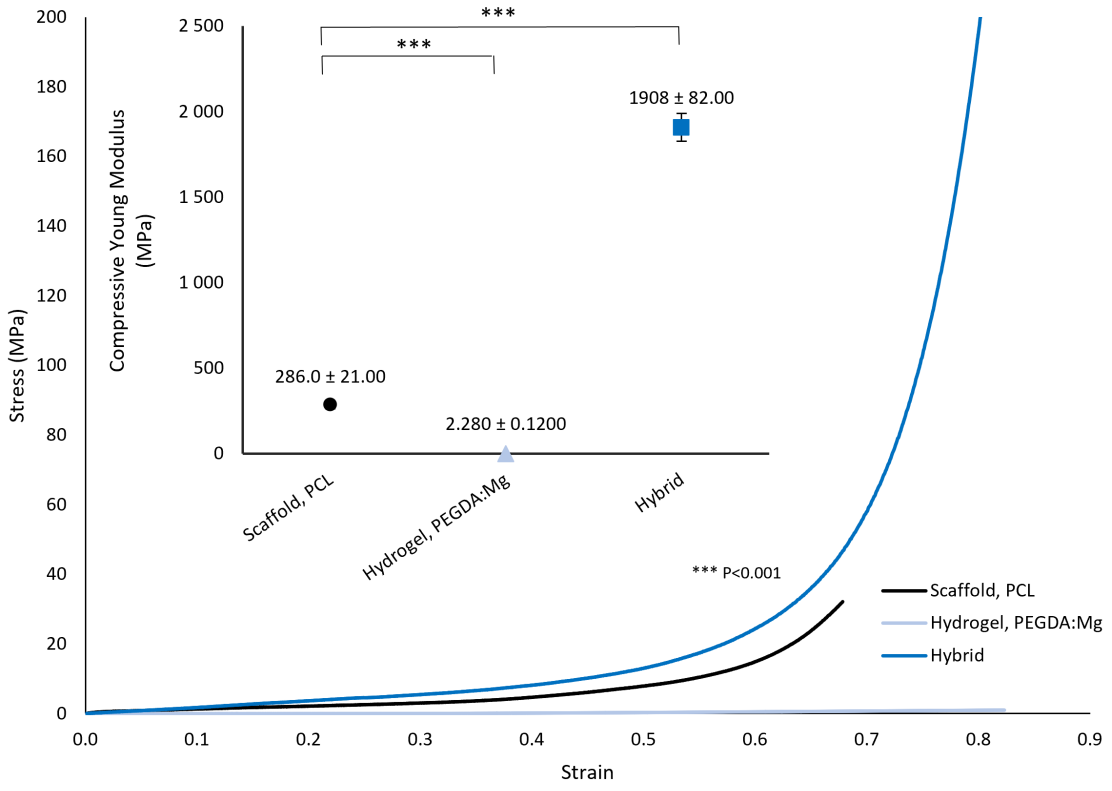

Figure 4.11: Mechanical behaviour of the three approaches: scaffold of PCL, hydrogel of PEGDA:Mg and hybrid strategy. Stress-strain curves and the compressive Young's Modulus (N = 5) are presented (***P < 0.001).

5

Conclusions and Future Perspectives

Bone fractures and losses often result in critical bone defects, prompting the search for effective solutions. While conventional approaches like grafts are commonly used, their limitations have sparked interest in biodegradable and bioresorbable implants. Notably, Mg constitutes a substantial portion of our body's composition. This work hypothesised that incorporating Mg into biomaterials augments their mechanical and biological properties, supporting the creation of new tissue while the implant gradually degrades.

3D structures were successfully produced through extrusion technique containing different contents of MgO and $MgSO_4$, hydrogels incorporating biologically active ions of Mg and a hybrid strategy combining the 3D structures without Mg (structural material) with a hydrogel with Mg ions (delivery vehicle of the bioactive compound).

The 3D AM structures were produced with the desired pore and filament size, presenting a rough surface with the introduction of Mg. Besides, it was confirmed that Mg was randomly integrated into the PCL matrix. Moreover, for this approach, a Mg content of 5% emerged as optimal, as it exhibited the highest resistance to compression across both forms of Mg, reflecting superior mechanical properties. Future work will involve exploring alternative methods for material formulation, avoiding the use of organic solvents. Additionally, there will be a focus on evaluating scaffold degradation rates while examining the release kinetics of Mg to avoid any toxic levels.

PEGDA-based hydrogels infused with biologically active Mg ions were also successfully developed. Our findings indicate that these hydrogels degrade gradually within hydrolytic environments, contributing to the controlled release of Mg ions, which may foster cell proliferation and support bone healing process. Additionally, in terms of mechanical attributes, the inclusion of Mg led to an enhancement of the hydrogels' mechanical properties. This was evidenced by increased resistance and elasticity under compression, ultimately yielding a higher compressive Young's Modulus. Upcoming research will entail a comprehensive comparison of the behaviour exhibited by synthetic and natural-based hydrogels upon Mg inclusion. Furthermore, cellular experiments would provide valuable insights into cell behaviour, encompassing aspects such as proliferation, growth, and bone formation.

Combining the two previously discussed structures, a hybrid strategy was also carried out, leading to outstanding mechanical properties. This resulted in a significant increase in the compressive Young's Modulus compared to the individual structures, reaching levels near the ones found in natural bone. In future studies, it would be interesting to assess the structure's porosity and explore cellular responses.

6

Scientific Outputs

Throughout this master thesis research, I have had the privilege of contributing to the scientific community through various research endeavours. Here, I will highlight some of my key contributions in the form of conference proceedings, poster and forthcoming publications.

Oliveira, B., Baptista, A. C., Malça, C., Coutinho, J., Henriques, M. and Moura, C. (2023). Magnesium-based biodegradable scaffolds for bone tissue regeneration presented at X Congress of the Portuguese Society of Biomechanics (X CNB'23), Feb 5-6, Figueira da Foz, Portugal.

Oliveira, B., Neves, J., Malça, C., Campos, S., Sá, J., Henriques, M., Baptista, A. and Moura, C. (2023). Hybrid hydrogel as a delivery vehicle for bioactive ions to enhance bone regeneration presented at the 12th Mechanical Technologies and Structural Materials (MTSM'23), Sep 21-22, Split, Croatia.

Campos, S., Sá, J., Oliveira, B., Malça, C. and Moura, C. (2023). Impact of the addition of magnesium oxide and magnesium sulphate on scaffolds to Bone Tissue Engineering presented at the IV Digital Conference on Nanobiotechnology and Bioengineering (CDNB'23), Jun 13-16, Online, Brazil.

I am excited to announce both conference participations will be published in SCOPUS index journals. These papers represent a significant milestone in my academic journey, and I look forward to sharing them with the scientific community once it is published.

Bibliography

[1] J. M. Lourenço. *The NOVAthesis LaTeX Template User's Manual*. NOVA University Lisbon. 2021. URL: https://github.com/joaomlourenco/novathesis/raw/master/template.pdf (cit. on p. iii).

[2] S. Singh et al. "Synthesis and characterization of a novel open cellular Mg-based scaffold for tissue engineering application". In: *Journal of the Mechanical Behavior of Biomedical Materials* 94 (2019-06), pp. 54–62. ISSN: 18780180. DOI: 10.1016/j.jmbbm.2019.02.010 (cit. on pp. 1, 17).

[3] S. Biscaia et al. "Additive Manufactured Poly(ϵ-caprolactone)-graphene Scaffolds: Lamellar Crystal Orientation, Mechanical Properties and Biological Performance". In: *Polymers* 14 (9 2022-05). ISSN: 20734360. DOI: 10.3390/polym14091669 (cit. on pp. 1, 2).

[4] N. E. Putra et al. *Multi-material additive manufacturing technologies for Ti-, Mg-, and Fe-based biomaterials for bone substitution*. 2020-06. DOI: 10.1016/j.actbio.2020.03.037 (cit. on pp. 1, 5, 6).

[5] A. H. Schmidt. "Autologous bone graft: Is it still the gold standard?" In: *Injury* 52 (2021-06), S18–S22. ISSN: 18790267. DOI: 10.1016/j.injury.2021.01.043 (cit. on p. 1).

[6] C Delloye et al. "Aspects of current management Bone allografts what they can offer and what they cannot". In: *The journal of bone and joint surgery* (2007). DOI: 10.1302/0301-620X.89B5 (cit. on p. 1).

[7] S. Zhao et al. "Fabrication and Biological Activity of 3D-Printed Polycaprolactone/Magnesium Porous Scaffolds for Critical Size Bone Defect Repair". In: *ACS Biomaterials Science and Engineering* 6 (9 2020-09), pp. 5120–5131. ISSN: 23739878. DOI: 10.1021/acsbiomaterials.9b01911 (cit. on pp. 1, 2, 8, 19, 20).

[8] P. R. Gabbai-Armelin et al. "Effects of bio-inspired bioglass/collagen/magnesium composites on bone repair". In: *Journal of Biomaterials Applications* 34 (2 2019-08), pp. 261–272. ISSN: 15308022. DOI: 10.1177/0885328219845594 (cit. on pp. 1, 5).

[9] A. Abdal-hay et al. "Fabrication of biocompatible and bioabsorbable polycaprolactone/ magnesium hydroxide 3D printed scaffolds: Degradation and in vitro osteoblasts interactions". In: *Composites Part B: Engineering* 197 (2020-09). ISSN: 13598368. DOI: 10.1016/j.compositesb.2020.108158 (cit. on pp. 1, 7, 8, 19, 20).

[10] Y. Tang et al. "In situ gas foaming based on magnesium particle degradation: A novel approach to fabricate injectable macroporous hydrogels". In: *Biomaterials* 232 (2020-02). ISSN: 18785905. DOI: 10.1016/j.biomaterials.2019.119727 (cit. on pp. 1, 2, 9).

[11] M. H. Kang et al. "Biomimetic porous Mg with tunable mechanical properties and biodegradation rates for bone regeneration". In: *Acta Biomaterialia* 84 (2019-01), pp. 453–467. ISSN: 18787568. DOI: 10.1016/j.actbio.2018.11.045 (cit. on pp. 1, 7).

[12] P. Xiong et al. "A pH-sensitive self-healing coating for biodegradable magnesium implants". In: *Acta Biomaterialia* 98 (2019-10), pp. 160–173. ISSN: 18787568. DOI: 10.1016/j.actbio.2019.04.045 (cit. on pp. 1, 6).

[13] K. Zhang et al. "Nanocomposite hydrogels stabilized by self-assembled multivalent bisphosphonate-magnesium nanoparticles mediate sustained release of magnesium ion and promote in-situ bone regeneration". In: *Acta Biomaterialia* 64 (2017-12), pp. 389–400. ISSN: 18787568. DOI: 10.1016/j.actbio.2017.09.039 (cit. on p. 1).

[14] M. Yin et al. "Incorporation of magnesium ions into photo-crosslinked alginate hydrogel enhanced cell adhesion ability". In: *Journal of Tissue Engineering and Regenerative Medicine* 9 (9 2015-09), pp. 1088–1092. ISSN: 19327005. DOI: 10.1002/term.2011 (cit. on pp. 1, 9).

[15] B. Chen et al. "Enhancement of critical-sized bone defect regeneration by magnesium oxide-reinforced 3D scaffold with improved osteogenic and angiogenic properties". In: *Journal of Materials Science and Technology* 135 (2023-02), pp. 186–198. ISSN: 10050302. DOI: 10.1016/j.jmst.2022.06.036 (cit. on pp. 1, 6, 8).

[16] H. S. Roh et al. "Addition of MgO nanoparticles and plasma surface treatment of three-dimensional printed polycaprolactone/hydroxyapatite scaffolds for improving bone regeneration". In: *Materials Science and Engineering C* 74 (2017-05), pp. 525–535. ISSN: 09284931. DOI: 10.1016/j.msec.2016.12.054 (cit. on pp. 1, 6, 7, 21).

[17] C. M. Murphy, M. G. Haugh, and F. J. O'Brien. "The effect of mean pore size on cell attachment, proliferation and migration in collagen-glycosaminoglycan scaffolds for bone tissue engineering". In: *Biomaterials* 31 (3 2010-01), pp. 461–466. ISSN: 01429612. DOI: 10.1016/j.biomaterials.2009.09.063 (cit. on pp. 2, 17).

[18] S. H. Teoh, B. T. Goh, and J. Lim. *Three-Dimensional Printed Polycaprolactone Scaffolds for Bone Regeneration Success and Future Perspective*. 2019-07. DOI: 10.1089/ten.tea.2019.0102 (cit. on p. 2).

[19] J. Dong et al. "Solvent-cast 3D printing of magnesium scaffolds". In: *Acta Biomaterialia* 114 (2020-09), pp. 497–514. ISSN: 18787568. DOI: 10.1016/j.actbio.2020.08.002 (cit. on pp. 2, 5, 6).

[20] M. G. Raucci, V. Guarino, and L. Ambrosio. "Hybrid composite scaffolds prepared by sol-gel method for bone regeneration". In: *Composites Science and Technology* 70 (13 2010-11), pp. 1861–1868. ISSN: 02663538. DOI: 10.1016/j.compscitech.2010.05.030 (cit. on p. 2).

[21] I. Manavitehrani et al. "Formation of porous biodegradable scaffolds based on poly(propylene carbonate) using gas foaming technology". In: *Materials Science and Engineering C* 96 (2019-03), pp. 824–830. ISSN: 18730191. DOI: 10.1016/j.msec.2018.11.088 (cit. on p. 2).

[22] Z. Fereshteh. "Freeze-drying technologies for 3D scaffold engineering". In: Elsevier, 2018, pp. 151–174. ISBN: 9780081009802. DOI: 10.1016/B978-0-08-100979-6.00007-0 (cit. on p. 2).

[23] K. Y. Tsai et al. "Laser sintered magnesium-calcium silicate/poly-ϵ-caprolactone scaffold for bone tissue engineering". In: *Materials* 10 (1 2017). ISSN: 19961944. DOI: 10.3390/ma10010065 (cit. on p. 2).

[24] P. Marcelino et al. "A Novel Approach for Design and Manufacturing of Curvature-Featuring Scaffolds for Osteochondral Repair". In: *Polymers* 15 (9 2023-05). ISSN: 20734360. DOI: 10.3390/polym15092129 (cit. on p. 2).

[25] Z. Yao et al. "Magnesium-Encapsulated Injectable Hydrogel and 3D-Engineered Polycaprolactone Conduit Facilitate Peripheral Nerve Regeneration". In: *Advanced Science* 9 (21 2022-07). ISSN: 21983844. DOI: 10.1002/advs.202202102 (cit. on p. 2).

[26] N. E. Fedorovich et al. "The effect of photopolymerization on stem cells embedded in hydrogels". In: *Biomaterials* 30 (3 2009-01), pp. 344–353. ISSN: 01429612. DOI: 10.1016/j.biomaterials.2008.09.037 (cit. on p. 2).

[27] K. T. Nguyen and J. L. West. *Photopolymerizable hydrogels for tissue engineering applications*. 2002 (cit. on p. 2).

[28] E. Nicol. *Photopolymerized Porous Hydrogels*. 2021-04. DOI: 10.1021/acs.biomac.0c01671 (cit. on p. 2).

[29] L. Claes, S. Recknagel, and A. Ignatius. *Fracture healing under healthy and inflammatory conditions*. 2012-03. DOI: 10.1038/nrrheum.2012.1 (cit. on pp. 5, 24).

[30] M. S. Ghiasi et al. *Bone fracture healing in mechanobiological modeling: A review of principles and methods*. 2017-06. DOI: 10.1016/j.bonr.2017.03.002 (cit. on pp. 5, 24).

[31] L. C. Gerhardt and A. R. Boccaccini. "Bioactive glass and glass-ceramic scaffolds for bone tissue engineering". In: *Materials* 3 (7 2010), pp. 3867–3910. ISSN: 19961944. DOI: 10.3390/ma3073867 (cit. on pp. 5, 25).

[32] V. Karageorgiou and D. Kaplan. *Porosity of 3D biomaterial scaffolds and osteogenesis*. 2005. DOI: 10.1016/j.biomaterials.2005.02.002 (cit. on pp. 5, 25).

[33] N. Sezer, Z. Evis, and M. Koç. *Additive manufacturing of biodegradable magnesium implants and scaffolds: Review of the recent advances and research trends*. 2021-03. DOI: 10.1016/j.jma.2020.09.014 (cit. on p. 6).

[34] M. Fernandes et al. "AML_Volume 11_Issue 8_Pages 1-10". In: (2020) (cit. on p. 6).

[35] *Magnesium Sulfate and Bupivacaine for Rehabilitation After Distal Radius Fractures - Full Text View - ClinicalTrials.gov*. URL: https://classic.clinicaltrials.gov/ct2/show/NCT02514343 (cit. on p. 6).

[36] K. S. Park et al. "Versatile effects of magnesium hydroxide nanoparticles in PLGA scaffold–mediated chondrogenesis". In: *Acta Biomaterialia* 73 (2018-06), pp. 204–216. ISSN: 18787568. DOI: 10.1016/j.actbio.2018.04.022 (cit. on pp. 7, 8).

[37] Y. Chen et al. "A Composite of Cubic Calcium-Magnesium Sulfate and Bioglass for Bone Repair". In: *Frontiers in Bioengineering and Biotechnology* 10 (2022-06). ISSN: 22964185. DOI: 10.3389/fbioe.2022.898951 (cit. on p. 7).

[38] S. H. Wang et al. "Surface modification of biodegradable Mg-based scaffolds for human mesenchymal stem cell proliferation and osteogenic differentiation". In: *Materials* 14 (2 2021-01), pp. 1–18. ISSN: 19961944. DOI: 10.3390/ma14020441 (cit. on p. 8).

[39] H. A. Almeida et al. "Portuguese Patent no. 104247". Pat. 2010 (cit. on p. 12).

[40] *Effects of magnesium on skeletal metabolism - PubMed*. URL: https://pubmed.ncbi.nlm.nih.gov/2184830/ (cit. on p. 12).

[41] F. J. O'Brien. *Biomaterials & scaffolds for tissue engineering*. 2011 (cit. on p. 17).

[42] I. Castilla-Cortázar et al. "Morphology, crystallinity, and molecular weight of poly(ϵ-caprolactone)/graphene oxide hybrids". In: *Polymers* 11 (7 2019). ISSN: 20734360. DOI: 10.3390/polym11071099 (cit. on p. 21).

[43] R. Longo et al. "Thermal and mechanical characterization of complex electrospun systems based on polycaprolactone and gelatin". In: *Journal of Thermal Analysis and Calorimetry* 147 (9 2022-05), pp. 5391–5399. ISSN: 15882926. DOI: 10.1007/s10973-022-11225-7 (cit. on p. 21).

[44] M. A. Ahmed and Z. M. Abou-Gamra. "Mesoporous MgO nanoparticles as a potential sorbent for removal of fast orange and bromophenol blue dyes". In: *Nanotechnology for Environmental Engineering* 1 (1 2016-12). ISSN: 23656387. DOI: 10.1007/s41204-016-0010-7 (cit. on p. 21).

[45] M. Suardi et al. "Formulation of urea microcapsules by using Polystyrene:Polycaprolactone matrix and its characterization". In: *International Research Journal Of Pharmacy* 9 (11 2018-12), pp. 42–47. DOI: 10.7897/2230-8407.0911255 (cit. on p. 21).

[46] G. Balakrishnan et al. "Microstructure, optical and photocatalytic properties of MgO nanoparticles". In: *Results in Physics* 16 (2020-03). ISSN: 22113797. DOI: 10.1016/j.rinp.2020.103013 (cit. on p. 21).

[47] V. G. Vyatchina et al. "Structure and properties of glasses in the MgSO4-Na 2B4O7-KPO3 system". In: *Glass Physics and Chemistry* 35 (6 2009-12), pp. 580–585. ISSN: 10876596. DOI: 10.1134/S1087659609060054 (cit. on p. 21).

[48] V. B. Morris et al. "Mechanical Properties, Cytocompatibility and Manufacturability of Chitosan:PEGDA Hybrid-Gel Scaffolds by Stereolithography". In: *Annals of Biomedical Engineering* 45 (1 2017-01), pp. 286–296. ISSN: 15739686. DOI: 10.1007/s10439-016-1643-1 (cit. on p. 22).

[49] K. O'Donnell, A. Boyd, and B. J. Meenan. "Controlling fluid diffusion and release through mixed-molecular-weight poly(ethylene) glycol diacrylate (PEGDA) hydrogels". In: *Materials* 12 (20 2019-10). ISSN: 19961944. DOI: 10.3390/ma12203381 (cit. on p. 22).

[50] R. Rothe et al. "Adjuvant drug-assisted bone healing: Part I-Modulation of inflammation". In: *Clinical Hemorheology and Microcirculation* 73 (3 2020), pp. 381–408. ISSN: 18758622. DOI: 10.3233/CH-199102 (cit. on p. 24).

[51] A. Remedios. *Bone and bone healing*. 1999. DOI: 10.1016/S0195-5616(99)50101-0 (cit. on p. 24).

A

Compressive Young's Modulus

It is presented the compressive Young's Modulus of the several approaches studied.

Table A.1: Compressive Young's Modulus of discs.

Group	***Compressive Young's Modulus (MPa)***
PCL	96.0±26.0
5% MgO	133±47.0
10% MgO	92.0±13.0
15% MgO	106±62.0
5% $MgSO_4$	157±4.00
10% $MgSO_4$	91.0±9.00
15% $MgSO_4$	89.0±25.0

Table A.2: Compressive Young's Modulus of 3D AM scaffolds.

Group	***Compressive Young's Modulus (MPa)***
PCL	286±21.0
5% MgO	282±41.0
15% MgO	193±31.0
5% $MgSO_4$	291±25.0
15% $MgSO_4$	233±31.0

Table A.3: Compressive Young's Modulus of hydrogels.

Group	***Compressive Young's Modulus (MPa)***
PEGDA	1.85±0.200
PEGDA:Mg	2.28±0.120

Table A.4: Compressive Young's Modulus of hybrid strategy.

Group	***Compressive Young's Modulus (MPa)***
Scaffold PCL	286.0±21.00
Hydrogel PEGDA:Mg	2.280±0.1200
Hybrid Strategy	1908±82.00

B

Compression of scaffolds, SEM images

It is presented SEM images, with a magnification of x50, for the 3D AM scaffolds after compression.

Table B.1: Cross-sectional view of SEM images of the produced scaffolds after compression.

Group	*Cross-sectional view of compressed scaffolds (50x)*	*Group*	*Cross-sectional view of compressed scaffolds (50x)*
PCL	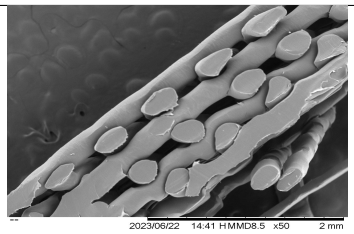		
5% MgO	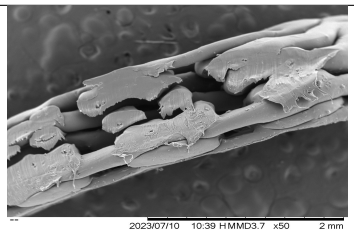	5% $MgSO_4$	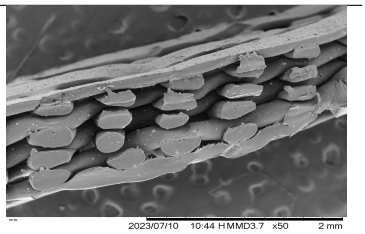
15% MgO	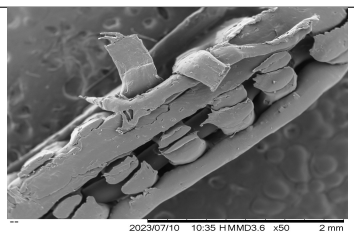	15% $MgSO_4$